HYBRID SENSORLESS CONTROL OF PMSM IN FULL SPEED RANGE USING HFI AND BACK-EMF

Slimane Medjmadj*

ETA Laboratory, Faculty of Sciences and Technology, University of Bordj Bou Arreridj, Algeria.

ARTICLE INFO

***Article history*:**
Received: 25.02.2023
Received in revised form: 28.04.2023.
Accepted: 10.05.2023.

Keywords:

Sensorless control
Back-EMF
PMSM
High frequency injection
Hybrid controller

DOI: 10.30765/er.2103

Abstract:

The permanent magnet synchronous motors (PMSM) are more and more used because of their high performance compared with other AC motors. The present paper proposes a hybrid controller which consists of a high frequency injection estimator and a back-electromotive-force observer in full speed range for the sensorless control of PMSM. The aim objective of the study to prevent speed overshot in startup time of the motor and provides a better dynamic response in transient and permanent states using this structure. A hybrid algorithm is applied to realize a smooth transition from low to high speed. At standstill and very low speed region, HF injection technique is used to detect the rotor initial position. In this first step study, the position estimation is derived from a HF current injection by using only one filter. When the rotor speed goes up to a certain value where back-EMF can provide adequate information, a back-EMF observer will dominate. Thanks to this structure, the mechanical sensor can be engaged using the best estimates and the developed control method is fast, simple, and flexible. The effectiveness, superiority, and performance of the proposed control method and extensive simulation results are provided on a 1 kW permanent magnet synchronous motor drive, demonstrating the expected performances.

1 Introduction

Over the past decades, numerous control strategies have been developed for electric drives control to ensure high precision and less complexity [1]. A novel concept for multi-motor drive systems, based on utilisation of multi-phase machines and inverters, has been proposed recently in [2]. Currently, permanent magnet synchronous motor (PMSM) drives are replacing classic dc and induction machine drives in a variety of industrial applications. Due to the advantages in efficiency, power density, reliability and so on, permanent magnet synchronous motor (PMSM) has been considered to have great potential to compete with the asynchronous motor in electric drive system and other application areas.

The sensorless concept has been well researched in the literature for the past four decades. Many advantages of sensorless AC drives such as reduced size, reduced hardware complexity, low cost, increased noise immunity, cable elimination, increased reliability and decreased maintenance. These approaches can be classified into two categories: the fundamental model-based methods for high-speed range and the high frequency injection (HFI) method based on the saliency for low-speed range.

The fundamental-model-based methods are available in the medium- and high speed ranges, while the saliency-based methods are able to track the position at standstill and low-speed ranges [3]. Based on when the high frequency carrier signal is injected, the HFI schemes can be further divided into two approaches, which are; stationary reference frame injection and synchronous reference frame injection.
These schemes are more suitable for the zero and low speed regions as the techniques used are independent of motor parameters. Herein, we address both existing problematic:

* Corresponding author
E-mail address: s.medjmadj@univ-bba.dz

- Ensure stable and robust motor operation in the low speed area without a mechanical sensor;
- Reach comparable level of performance between operation with sensor and without sensor at low and zero speed.

There are several works and methods to implement the speed sensorless controller in the literature, these include; adaptive fuzzy robust control [4]; model reference adaptive system (MRAS) [5]; sliding mode observer [6], extended kalman filter [7]; direct torque control [8]; HFI methods [9], etc. Due to the problem at zero speed estimation for these methods which is based on the model-based techniques of the machine, the fundamental component model technique relies on the position and velocity dependency of the back-electromotive-force (back-EMF) [10] of the motor. These techniques present a general problem at standstill, the back electromotive force [10-11], is zero amplitude when the machine rotates at low speed, so we cannot distinguish between the real component of the back-EMF and noise signal.

The back-EMF based sensorless algorithm is mature enough and has already been combined with vector control strategy in industrial applications. The performance of the back-EMF based sensorless vector control is mainly determined by the sensorless algorithms with respect to the position and speed estimation. Recently, the back-EMF based methods are only intended to be operated in medium to high speed range [11]. In the low speed region as the back-EMF is reduced, the influence of parameter variations and measurement noise become more important. These effects can cause the performance of the model based schemes to degrade and at zero speed even become completely instable. To addresses the aforesaid problems, a hybrid sensorless control algorithm is proposed in this paper to control in full speed rang of PMSM drives. The main contribution of this work are to prevent speed overshot in start-up time of the motor and provides a better dynamic response in transient states. In addition, this study, in order to eliminate distortions caused by hybrid sensorless control method, due to its simplicity and good stability has been preferred for the estimation of the speed and position. In this paper, an improved (HFI - back-EMF) based hybrid sensorless control strategy is proposed, which overcomes the limitations of the conventional Back-EMF based algorithm at low and zero speeds ranges. Thanks to the usage of a HFI approach, the computational burden of the whole hybrid sensorless algorithm is reduced.

The proposed method is to show the strategy hybrid speed sensorless control (HSSC) for PMSM drives combining HFI [12-15] and Back-EMF [16-17] techniques over the full speed range. In this work, the transient and steady state performances of the proposed HSS control algorithm with the combination of a vector controller, two different virtual sensors: HFI estimator and and back-EMF observer, shows satisfactory results for all the previous performance indicators, which demonstrates the superiority and effectiveness of the proposed control method. This paper is organized as follows: Section 2 describes the control model and algorithms of PMSM drives using two different estimators: HFI estimator and back-electromotive-force observer and also employed hybrid speed sensorless control for PMSM. Section 3 gives a detailed description of the proposed scheme of the hybrid sensorless control algorithm. Section 4 shows the simulation results of the proposed hybrid sensorless scheme, and finally, some conclusions on this study are drawn in Section 5.

2 Model-based estimation and proposed hybrid sensorless combined HFI-BACK-EMF

2.1 The mathematical model of PMSM

The part describing the electrical dynamics can be expressed as [16]:

$$\begin{bmatrix} v_\alpha \\ v_\beta \end{bmatrix} = \begin{bmatrix} R_S & 0 \\ 0 & R_s \end{bmatrix} \begin{bmatrix} i_\alpha \\ i_\beta \end{bmatrix} + \rho \begin{bmatrix} L & 0 \\ 0 & L \end{bmatrix} \begin{bmatrix} i_\alpha \\ i_\beta \end{bmatrix} + \begin{bmatrix} e_\alpha \\ e_\beta \end{bmatrix} \tag{1}$$

Rs and L are stator resistance and inductance,

ρ is the differential operator

i and v are stator currents and voltages in $\alpha\beta$,

e_α , e_β :back-EMF and are given by.

$$\begin{cases} e_\alpha = -\psi_f w_e \sin\theta_e \\ e_\beta = -\psi_f w_e \cos\theta_e \end{cases} \quad (2)$$

$w_e = p w_r$, the electrical rotor angular velocity,

ψ_f : the flux linkage of permanent magnet and

θ_e : the electrical rotor position. Assume that the rotor speed changes slowly during the sample period, the back-EMF components:

$$\begin{cases} \dot{e}_\alpha = -w_e e_\beta \\ \dot{e}_\beta = -w_e e_\alpha \end{cases} \quad (3)$$

The equation of electromagnetic torque is:

$$T_{em} = J\dot{w} + B_m w + T_l \quad (4)$$

J: the moment of inertia, B_m: the coefficient of friction

The T_{em} can be simplified as follows with magnetic orientation control strategy $i_d = 0$:

T_{em} and T_l are electromagnetic torque and load tor

$$\dot{w} = -\frac{B_m}{J} w + \frac{C_m . \phi_m}{J} i_q - \frac{1}{J} T_l \quad (5)$$

C_m : the torque coefficient at rated flux.

2.2. HFI-Estimator

If L_d differs from L_q, it is possible to estimate the rotor position by superimposing to the low frequency excitation of the PMSM [18]. The stator voltage model in the dq is:

$$\begin{bmatrix} V_d \\ V_q \end{bmatrix} = \begin{bmatrix} R_s & 0 \\ 0 & R_s \end{bmatrix} \begin{bmatrix} i_d \\ i_q \end{bmatrix} + \begin{bmatrix} \rho & -w_r \\ w_r & \rho \end{bmatrix} \begin{bmatrix} \psi_d \\ \psi_q \end{bmatrix} \quad (6)$$

The magnetic flux is:

$$\begin{bmatrix} \psi_d \\ \psi_q \end{bmatrix} = \begin{bmatrix} L_d & 0 \\ 0 & L_q \end{bmatrix} \begin{bmatrix} i_d \\ i_q \end{bmatrix} + \begin{bmatrix} \psi_m \\ 0 \end{bmatrix} \quad (7)$$

Transforming (6) into the stationary reference frame (wr=0):

$$\begin{bmatrix} V_\alpha \\ V_\beta \end{bmatrix} = \begin{bmatrix} R_s & 0 \\ 0 & R_s \end{bmatrix} \begin{bmatrix} i_\alpha \\ i_\beta \end{bmatrix} + \begin{bmatrix} \rho & 0 \\ 0 & \rho \end{bmatrix} \begin{bmatrix} \psi_\alpha \\ \psi_\beta \end{bmatrix} \quad (8)$$

This voltage injection technique is often called "α, β" injection because the rotating voltage signal is applied in the stationary frame "α, β". Figure 1 shows the rotating voltage vector that is applied in the stator reference frame.

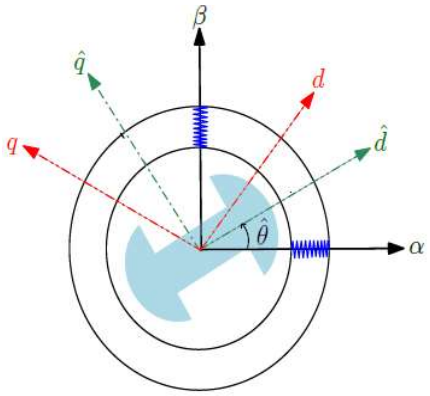

Figure 1. Rotating HFVI in the stationary reference frame.

The effects of the permanent magnet flux linkages and the stator resistance can be neglected for high frequency signals. The equations high frequency currents are [9]:

$$\begin{bmatrix} i_{\alpha i} \\ i_{\beta i} \end{bmatrix} = \begin{bmatrix} I_{i0}\cos(\omega_i t) + I_{i1}\cos(2\theta_r - \omega_i t) \\ I_{i0}\sin(\omega_i t) + I_{i1}\sin(2\theta_r - \omega_i t) \end{bmatrix} \tag{9}$$

With:

$$I_{i0} = \frac{V_{si}(L_q + L_d)}{2\omega_i L_q L_d} \quad ; \quad I_{i1} = \frac{V_{si}(L_q - L_d)}{2\omega_i L_q L_d}$$

Equation (9) proportional to the saliency (Lq-Ld) and contains on the rotor position information 2θr [9]. The $\hat{\theta}_r$ can be obtained by:

$$\hat{\theta}_r = \frac{1}{2} arctg\left(\frac{i_\beta}{i_\alpha}\right) \tag{10}$$

When a HF voltage is applied to the machine windings, the resulting HF current signal contains the rotor position information. By demodulating those currents, the rotor position can therefore be estimated [9]. In addition, electric power quality phenomenon basically incorporate unbalanced voltage and current flickers, harmonics, voltage sag, swell, and power interruptions [19]. In order to reduce the computational burden of the estimation, a simplified version is displayed in Figure 2. It consists of using only one fourth-order low-pass filter (LPF) and one rotation. The low-pass-filter is used to attenuate the low frequency excitation component.

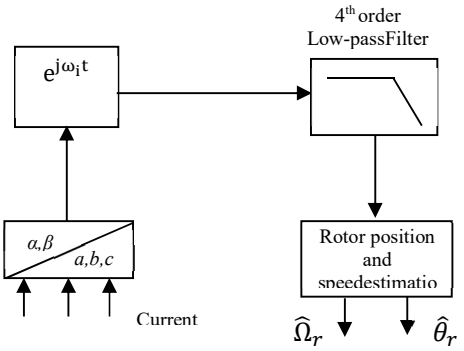

Figure 2. Simplified method for rotor position and speed estimations.

2.3. Back-EMF Observer

For purpose of a back-EMF observer, the salient PMSM is modelled as [19]:

$$\frac{d}{dt}\begin{bmatrix} i_{s\alpha} \\ i_{s\beta} \end{bmatrix} = \frac{1}{L_d}\begin{bmatrix} -R_s & -w(L_d - L_q) \\ w(L_d - L_q) & -R_s \end{bmatrix}\begin{bmatrix} i_{s\alpha} \\ i_{s\beta} \end{bmatrix} + \frac{1}{L_d}\begin{bmatrix} -1 & 0 \\ 0 & -1 \end{bmatrix}\begin{bmatrix} e_{s\alpha} \\ e_{s\beta} \end{bmatrix} + \frac{1}{L_d}\begin{bmatrix} v_{s\alpha} \\ v_{s\beta} \end{bmatrix} \tag{11}$$

With

$$\begin{bmatrix} e_{s\alpha} \\ e_{s\beta} \end{bmatrix} = \left(\left(L_d - L_q\right)\left(wi_{sd} - i_{sq}\right) + \psi w\right)\begin{bmatrix} -\sin\theta \\ \cos\theta \end{bmatrix} \tag{12}$$

Where (e) is the extended EMF.

$$\frac{d}{dt}\begin{bmatrix} \hat{i}_{s\alpha} \\ \hat{e}_{s\alpha} \end{bmatrix} = \frac{1}{L_d}\begin{bmatrix} -R_s & -1 \\ 0 & -0 \end{bmatrix}\begin{bmatrix} \hat{i}_{s\alpha} \\ \hat{e}_{s\alpha} \end{bmatrix} + \begin{bmatrix} k_{\alpha 1} \\ k_{\alpha 2} \end{bmatrix}\tilde{i}_{s\alpha} + \frac{1}{L_d}\begin{bmatrix} 1 \\ 0 \end{bmatrix}\left(v_{s\alpha} - \hat{w}(L_d - L_q)i_{s\beta}\right) \tag{13}$$

Figure 3 shows the relative positions of flux and back-EMF vectors in the αβ reference.

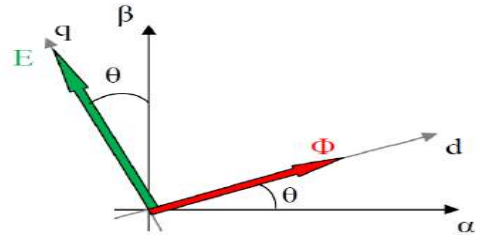

Figure 3. Flux and back-EMF vectors.

$$\frac{d}{dt}\begin{bmatrix} \hat{i}_{s\beta} \\ \hat{e}_{s\beta} \end{bmatrix} = \frac{1}{L_d}\begin{bmatrix} -R_s & -1 \\ 0 & -0 \end{bmatrix}\begin{bmatrix} \hat{i}_{s\beta} \\ \hat{e}_{s\beta} \end{bmatrix} + \begin{bmatrix} k_{\beta 1} \\ k_{\beta 2} \end{bmatrix}\tilde{i}_{s\beta} + \frac{1}{L_d}\begin{bmatrix} 1 \\ 0 \end{bmatrix}\left(v_{s\beta} - \hat{w}(L_d - L_q)i_{s\alpha}\right) \tag{14}$$

Where

$$\begin{cases} \tilde{i}_{s\alpha} = \hat{i}_{s\alpha} - i_{s\alpha} \\ \tilde{i}_{s\beta} = \hat{i}_{s\beta} - i_{s\beta} \end{cases} \tag{15}$$

In case of no salient $L_d = L_q = L$, the estimation errors is written as [20]:

$$\frac{d}{dt}\begin{bmatrix} \tilde{i}_{s\alpha} \\ \tilde{e}_{s\alpha} \end{bmatrix} = \begin{bmatrix} k_{\alpha 1} - \frac{R_s}{L} & -\frac{1}{L} \\ k_{\alpha 2} & 0 \end{bmatrix} \begin{bmatrix} \tilde{i}_{s\alpha} \\ \tilde{e}_{s\alpha} \end{bmatrix} \tag{16}$$

$$\frac{d}{dt}\begin{bmatrix} \tilde{i}_{s\beta} \\ \tilde{e}_{s\beta} \end{bmatrix} = \begin{bmatrix} k_{\beta 1} - \frac{R_s}{L} & -\frac{1}{L} \\ k_{\beta 2} & 0 \end{bmatrix} \begin{bmatrix} \tilde{i}_{s\beta} \\ \tilde{e}_{s\beta} \end{bmatrix} \tag{17}$$

Where

$$\begin{cases} \tilde{e}_{s\alpha} = \hat{e}_{s\alpha} - e_{s\alpha} \\ \tilde{e}_{s\beta} = \hat{e}_{s\beta} - e_{s\beta} \end{cases} \tag{18}$$

$k_{\alpha 1}, k_{\alpha 2}, k_{\beta 1}, k_{\beta 2}$ are the observer gains.

Using the Eq.(17), the estimated EEMF can be expressed as follows:

$$\begin{aligned} \dot{e}_{s\alpha} &= -\omega e_{s\beta} \\ \dot{e}_{s\beta} &= \omega e_{s\alpha} \end{aligned} \tag{19}$$

From Eq.(17), the adaptive EMF-observer is:

$$\begin{aligned} \dot{\hat{e}}_{s\alpha} &= -\hat{\omega}\hat{e}_{s\beta} - L\left(\hat{\hat{e}}_{s\alpha} - \hat{e}_{s\alpha}\right) \\ \dot{\hat{e}}_{s\beta} &= -\hat{\omega}\hat{e}_{s\alpha} - L\left(\hat{\hat{e}}_{s\beta} - \hat{e}_{s\beta}\right) \end{aligned} \tag{20}$$

Where L is a positive observer gain. The error dynamics are:

$$\begin{aligned} \dot{\tilde{e}}_{s\alpha} &= -\tilde{\omega}\hat{e}_{s\beta} - L\tilde{e}_{s\alpha} \\ \dot{\tilde{e}}_{s\beta} &= \tilde{\omega}\hat{e}_{s\alpha} - L\tilde{e}_{s\beta} \end{aligned} \tag{21}$$

2.4. Design of the hybrid sensorless controller combined HFI-BACK-EMF

The hybrid controller design for PMSM model plays a very important role in the operating system performance. This will guarantee complementary of operation in case of mechanical sensor loss or fault. The selection mechanism can be based on selection algorithms as shown in the block diagram below of Figure 4.

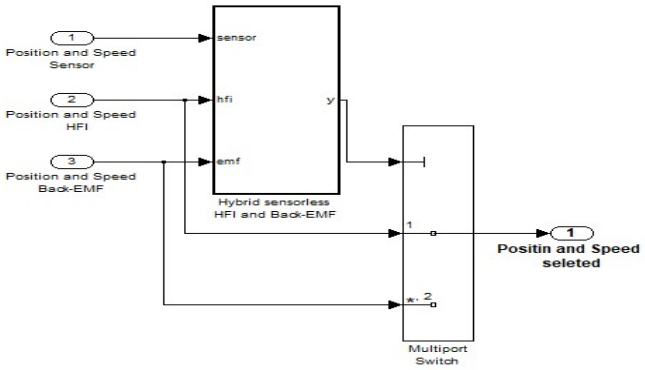

Figure 4. Block diagram of the Hybrid speed controller.

The hybrid sensorless will be based on the appropriate selection of estimators depending on the speed region as displayed in the following diagram. The operating point of the HFI estimator is set when $(\Omega \leq 10\%\,\Omega_n)$. Above 10% Ωn $(\Omega \rangle 10\%\Omega_n)$, only the back-EMF observer is used. The hybrid sensorless control model of PMSM is shown in Figure 5.

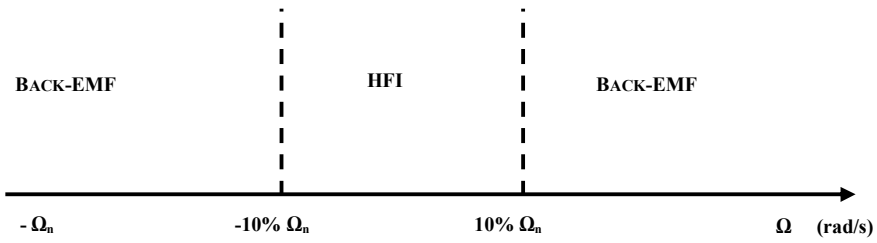

Figure 5. Combination of virtual sensors on the whole speed range.

3 Simulation results

The proposed hybrid sensorless vector control of PMSM by using HFI and back-EMF methods was simulated in Matlab/Simulink software. The PMSM is controlled by a PWM voltage source inverter using vector control strategy. The current control algorithm is carried out every 100 µs, and the speed control loop is carried out every 1ms. Tests are carried out under a load torque of 3.2 N.m. The parameters of the PMSM are listed in Table 1.

Table 1. PMSM Characteristics.

Symbol	Definition	Value
P_n	Nominal power	1.1 kW
Ω_n	Nominal speed	356 rad/s
T_n	Load torque	3.2 Nm
P	Pole pairs	3
I_n	Nominal current	5.9 A
Rs	Stator resistance	1.65 Ω
Ld	d axis inductance	3.5 10-3 H
Lq	q axis inductance	4.5 10-3 H
Ψ_m	Magnetic flux	154 10-3Wb
f	Viscous friction	509 10 -3 Nm/rad
J	Moment of inertia	6.4 10-3 kg/m²

The results of these tests are shown in Figure 6 for the HFI sensorless at 30rad/s. Figure 7 shows the speed and position wave forms of the proposed back-electromotive-force sensorless method at 157rad/s. Solid lines represent the actual rotor speed/position, and dashed lines represent the estimation. We can also notice the rapid convergence of the two estimations under load torque.

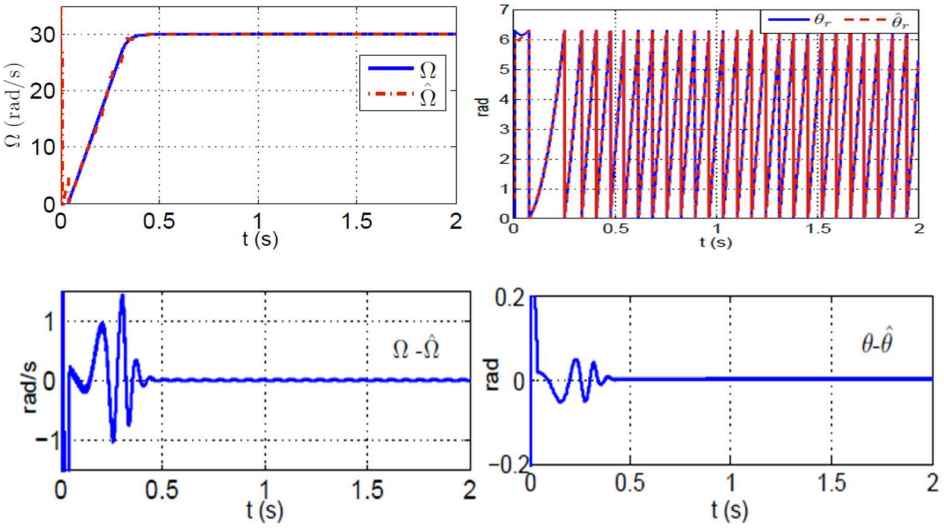

Figure 6. HFI sensorless simulation results at 30[rad/s] under load torque.

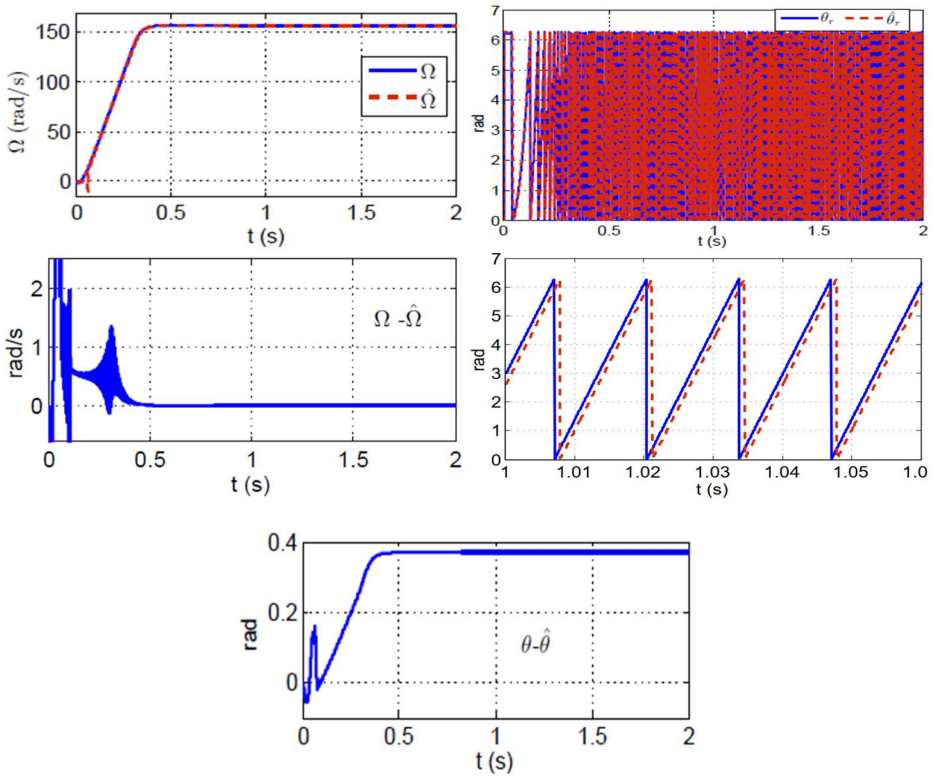

Figure 7. Back-EMF sensorless simulation results at 157[rad/s] under load torque.

To evaluate this hybrid sensorless control, from 0 to 10 at 157 rad/s and a nominal torque of 3.2 Nm is applied in this test. Figure 8 show the hybrid sensorless simulation results at full speed for PMSM under nominal torque (3.2 N.m) of measured speed, estimated speed and its errors, measured, estimated rotor electric position

and its errors, stator current components respectively. As seen from the Figure 8, the hybrid sensorless control is assumed from zero to 10 rad/s (corresponding from 0s to 1s), with high frequency voltage signal injection method; when exceeding 10% of the nominal speed (corresponding from 1s to 2s), only the back electromotive force observer works. The rotor electric position error is lower than 0.15rad. These results show the performances of the mechanical rotor speed and rotor electric position tracking capabilities of the hybrid sensorless.

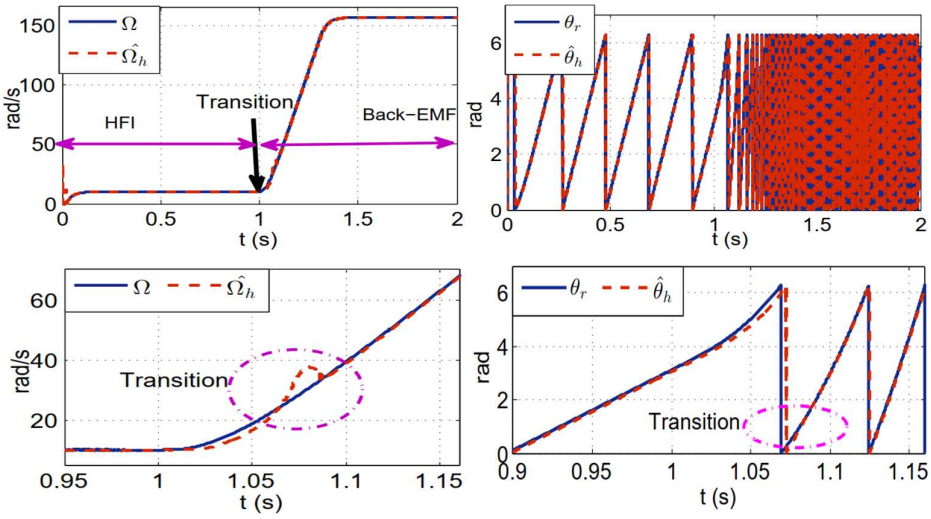

a) Mechanical speed and its estimation *c) Actual and estimated rotor position*

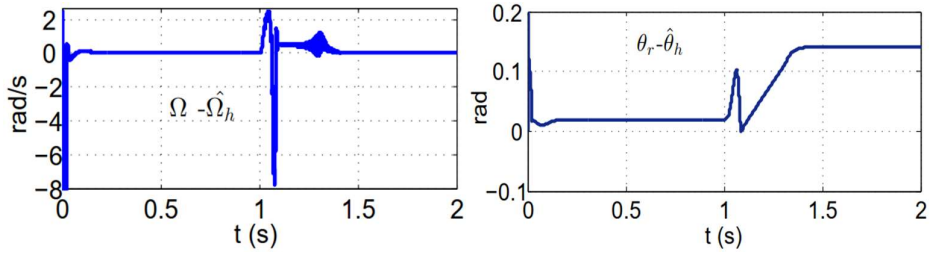

b) Mechanical speed estimation error *d) Rotor position errors*

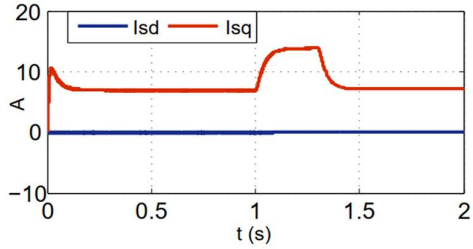

e) Stator currents compenents

Figure 8. Hybrid sensorless results at full speed for PMSM under nominal torque of the proposed control method.

For comparative analysis, every aspect of the simulation results is analyzed and visualized graphically. In order to cope with such challenges, a novel hybrid strategy of (HFI-EMF) is proposed that provides advantages over used in literature algorithms: fewer current ripples, short peak time, improved settling time, controlled overshoot regarding speed variations, and an overall improved estimation.

Simulation tests are performed to evaluate the robustness of the hybrid sensorless to the stator resistance Rs and inductance Lq variations on the whole operating range. An analytical study is derived to support the robustness assessment. Figure.9 we display the results of the hybrid sensorles robustness in case of permanent magnet synchronous motor drive parameter variations under load torque (2 Nm).

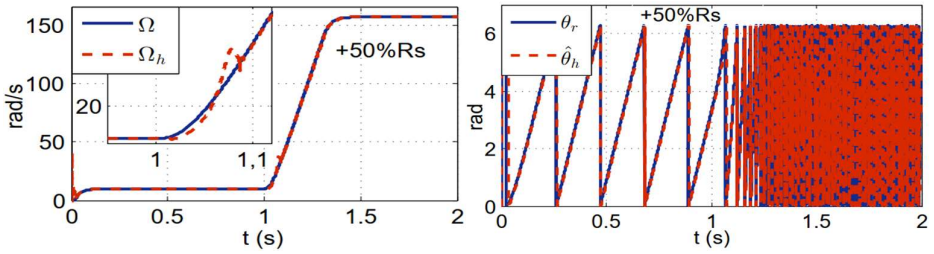

a) Speed and Position estimation under Rs variation (+50 %)

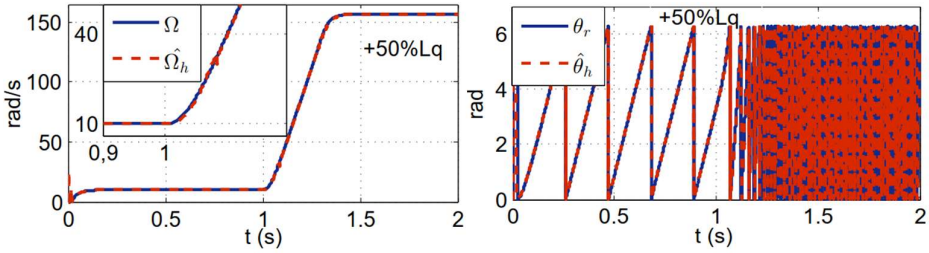

b) Speed and Position estimation under Lq variation (+50 %)

Figure 9. Hybrid sensorless robustness to parameter variations of PMSM under torque of the proposed control method.

As a conclusion, very acceptable results are obtained in simulation tests at different speed/torque ranges despite the variations of inductances and resistances, which confirms the machine parameters insensitivity of the procedure estimation strategy proposed. In general the overall estimate by the proposed method is simple, flexible and improved.

4 Conclusion

In this paper, we have investigated the possibility to implement a mechanical hybrid speed sensorless control for a PMSM drive system in full speed range. The proposed hybrid sensorless algorithm estimates the rotor position and speed are primarily divided into two categories: from a back-electromotive-force for medium and high speeds, together with a high frequency injection technique, which only works at zero or standstill and low speeds. The combining function provides a seamless transition between the HFI and the back-EMF schemes. This method is well-suited for startup processes at low speed and the transition to high speed of the sensorless control, which ensures a good robustness and adaptability of the whole control system. Simulation results show the feasibility of the proposed strategy, and confirm that the method is efficient at in full speed range and at standstill. In addition, hybrid sensorless control algorithm shows greater robustness to parameter variations than the traditional controller.

References

[1] A.O Salau, T.M Anteneh, "Direct Quadrate Modeling of a Direct Torque Control for a 3-Phase Induction Motor" , *6th International Conference on Signal Processing, Computing and Control (ISPCC),* pp. 522-527. DOI: 10.1109/ISPCC53510.2021.9609480, 2021.

[2] A.W Yesgat, A.O Salau , H.E Kasshun, "Fuzzy Based Sliding Mode Control of Vector controlled Multiphase Induction Motor Drive under Load Fluctuation", *Journal of Electrical and Electronics Engineering ;* Oradea,Vol. 15, N 2, pp.98-105, 2022.

[3] W Yang, H Guo , X Sun , Y Wang , S Riaz and H Zaman, "Wide-Speed-Range Sensorless Control of IPMSM", *Electronics MDPI,* Vol. 11(22), 3747, 2022.

[4] Xingjian Wang, Shaoping Wang, "Adaptive fuzzy robust control of PMSM with smooth inverse based dead-zone compensation", *International Journal Of Control, Automation, and Systems*, Vol. 14, No. 2, pp.378-388, 2016. https://Doi.Org/10.1007/S12555-015-0010-6

[5] A.Mishra , V. Mahajan, Et Al, "MRAS based estimation of speed in sensorless pmsm drive", *Ieee Fifth Power India Conference,* 19-22 December 2012, Murthal, India; Doi: 10.1109/Poweri.2012.6479492

[6] Y. Zhan, J. Guan, Y. Zhao, "An adaptive second-order sliding-mode observer for permanent magnet synchronous motor with an improved phase-locked loop structure considering speed reverse", *Transactions Of The Institute Of Measurement And Control,* November 4, 2019. Doi:10.1177/0142331219880712

[7] K. Kyslan, V. Slapak, V. Petro, A. Marcinek, F. Durovsky, "Speed sensorless control of PMSM with unscented Kalman Filter and Initial Rotor," *International Conference On Electrical Drives & Power Electronics (Edpe), The High Tatras*, 24-26 Sept. 2019. Doi: 10.1109/Edpe.2019.8883918

[8] T.M Anteneh, A.O Salau, T.F Agajie, E.A Hailu, "Design and implementation of a Direct Torque Controller for a Three Phase Induction Motor based on DSP", *International Journal of Applied Engineering Research,* Vol. 14(22), pp. 4181-4187, 2019.

[9] S. Medjmadj, D. Diallo, M. Mostefai, C. Delpha And A. Arias, "PMSM drive position estimation: contribution to the high-frequency injection voltage selection issue", *Ieee Transactions On Energy Conversion,* Vol. 30, No.1, Pp. 349-358, Mar. 2015. Doi:10.1109/Tec.2014.2354075

[10] Jin-Woo Lee, "Adaptive Sensorless Control of High Speed PMSM with Back EMF Constant Variation," *9th International Conference on Power Electronics-ECCE Asia*. June 1 - 5, 63 Convention Center, Seoul, Korea, 2015.

[11] C. Zaghrini, G. Khoury, M. Fadel , R. Ghosn, F. Khatounian, "Adapted back-emf sensorless control for permanent magnet synchronous motors," *Ieee International Conference On Industrial Technology (Icit)* Melbourne, Australia, 13-15 Feb. 2019. Doi:10.1109/Icit39983.2019

[12] A. Arias, C. Silva, Gm. Asher, Jc. Clare, Pw. Wheeler, "Use of a matrix converter to enhance the sensorless control of a surface-mount permanent-magnet ac motor at zero and low frequency", *IEEE Trans Ind Electron, 53* (2), Pp. 440–449.

[13] J-S. Kim, S-K. Sul, "High performance PMSM drives without rotational position sensors using reduced order observer", *Industry Applications Conference", Conference Record of The IEEE;* 1995. Pp 75–82.
Doi:10.1109/Ias.1995.530286

[14] Cs. Staines, C. Caruana, Gm. Asher, And M. Sumner, "Sensorless control of induction machines at zero and low frequency using zero sequence currents", *IEEE Trans Ind Electron* 2006; 53(1):195–206. Doi:10.1109/Tie.2005.862295

[15] A. Arias, O. Caelos, Z. Jordi, J. Espina, And J. Pou, "Hybrid sensorless permanent magnet synchronous machine four quadrant drive based on direct matrix converter, " *International Journal Of Electrical Power & Energy Systems* 45(1):78–86, February 2013.
Doi: 10.1016/J.Ijepes.2012.08.073

[16] M. Nicola, C. Nicola, A. Vintila, "Sensorless control of multi-motors PMSM using back-emf sliding mode observer, "*Electric Vehicles International Conference (Ev),* Bucharest, Romania, Romania, 3-4 Oct. 2019. Doi**:** 10.1109/Ev.2019.8892950

[17] L. Kaiyuan, L. Xiao, And F. Blaabjerg, "Artificial inductance concept to compensate nonlinear inductance effects in the back emf-based sensorless control method for PMSM, " *IEEE Trans. Energy Convers.,* Vol. 28(3), Pp. 593–600, Sep. 2013. Doi: 10.1109/Tec.2013.2261995

[18] C. Ortega, A. Arias, C. Caruana, C. Staines, J. Balcells, J. Cilia, "Sensorless direct torque control of a surface mounted pmsm using high frequency injection," *IEEE International Symposium On Industrial Electronics*, Montreal, Quebec, Canada, July 2006, pp. 2332-2337.

Doi: 10.1109/Isie.2006.295937, 09-13 July 2006.

[19] C.U. Eya, A.O. Salau, and S.E. Oti, "Constant and wireless controlled DC-to-AC based boost differential converter with a sensor-less changeover system", *Int J Syst Assur Eng Manag*. DOI: 10.1007/s13198-021-01451-x, 2021.

[20] Z. Chen, M. Tomita, S. Doki, And S. Okuma, "An extended electromotive force model for sensorless control of interior permanent magnet synchronous motors," *IEEE Trans. Ind. Electron,* Vol. 50, No. 2, pp. 288–295. Doi: 10.1109/Tie.2003.809391, Apr 2003.